Gastroenterology Report, 2025, **13**, goaf024
https://doi.org/10.1093/gastro/goaf024
Original Article

Original Article

USP38 protects intestinal epithelial cells from ischemia/reperfusion injury by stabilizing BIRC5

Mandong Pan[1], Xianwei Huang[1], Xiaodong Huang[1], Xiong Liu[1] and Jiyan Lin[1,2,*]

[1]Emergency Department, The First Affiliated Hospital of Xiamen University, Xiamen, Fujian, P. R. China
[2]Xiamen Key Laboratory for Clinical Efficacy and Evidence-Based Research of Traditional Chinese Medicine, Xiamen, Fujian, P. R. China

*Corresponding author. Emergency Department, The First Affiliated Hospital of Xiamen University, No. 55 Zhenhai Road, Xiamen, Fujian 361003, China. Tel: +86-15980882638; Email: happylinjiy@163.com

Abstract

Background: Intestinal ischemia/reperfusion (II/R) is a severe condition with high mortality and limited treatment options. Extracellular vesicles that are derived from bone marrow mesenchymal stem cells (BM-MSC-EVs) exhibit therapeutic potential in alleviating II/R injury. However, the mechanism by which BM-MSC-EVs fulfill this function requires further characterization. The ubiquitin–proteasome system plays an essential role in II/R, but the functions of individual ubiquitination regulators such as ubiquitin-specific proteases (USPs) in this process remain incompletely understood.

Methods: An II/R cellular model was established by using IEC-6 intestinal epithelial cells with oxygen-glucose deprivation/reperfusion (OGD/R) treatment. The expression of USPs was evaluated by using quantitative polymerase chain reaction and Western blot. The role of USP38 on the viability, apoptosis, migration, and reactive oxygen species (ROS) levels in OGD/R-treated IEC-6 cells were measured by using CCK-8, Annexin V/PI staining, transwell assay, and 2′,7′-dichlorofluorescin diacetate (DCFDA) staining, respectively. The interaction between USP38 and BIRC5 was explored by using co-immunoprecipitation (Co-IP) and the ubiquitination level and stability of BIRC5 were examined by using Western blot. USP38-overexpressing BM-MSC-EVs were produced to treat OGD/R-treated IEC-6 cells.

Results: USP38 expression was significantly downregulated in OGD/R-treated IEC-6 cells. Incubation of these cells with BM-MSC-EVs substantially elevated the USP38 expression, resulting in improved viability, reduced apoptosis, enhanced migration, and decreased ROS levels. Furthermore, overexpression of USP38 in BM-MSC-EVs further enhanced their protective effect on OGD/R-treated IEC-6 cells. At the molecular level, USP38 interacts with and stabilizes BIRC5 by decreasing its ubiquitination. Knock-down of BIRC5 abolished the protective effect of excessive USP38 on OGD/R-treated IEC-6 cells.

Conclusion: USP38 protects intestinal epithelial cells from I/R injury by enhancing the stability of BIRC5.

Keywords: bone marrow mesenchymal stem cells (BM-MSCs); extracellular vesicle; intestinal ischemia/reperfusion (II/R); IEC-6 cells; USP38; BIRC5

Introduction

Intestinal ischemia/reperfusion (II/R) is a life-threatening condition that is associated with multiple risk factors, including severe trauma, small bowel transplantation, intestinal torsion, and hemorrhagic shock [1, 2]. II/R not only causes local intestinal barrier defects, but may also trigger systemic inflammation and multi-organ failure, making it a leading cause of death in patients with critical illness [3]. The injury that is caused by II/R can be divided into two phases: the initial ischemia and the subsequent reperfusion. During the ischemia phase, tissue damage is caused by hypoxia and is locally restricted. In the following reperfusion phase, reoxygenation prompts damaged tissues to generate a large amount of reactive oxygen species (ROS), triggering an oxidative stress response and the release of inflammatory factors. This process expands the damage distantly, exacerbating the overall injury [1, 4].

Currently, options for II/R treatment are limited and surgical intervention with supportive intensive care is considered the only effective treatment [2, 5]. Antioxidant-based therapy has shown a protective effect in II/R animal models [6, 7] but its effectiveness needs further validation in II/R patients. Therefore, the finding of novel therapies for II/R is urgently needed to improve the prognoses of II/R patients.

Stem-cell-based therapies have demonstrated significant potential in treating various medical conditions, including injuries caused by I/R [8–10]. They can also substantially alleviate the damage that is triggered by II/R [11, 12]. However, the application of stem-cell-based therapies is constrained by factors such as ethical concerns, limited stem-cell resources, and immunogenicity [13]. In comparison, extracellular vesicles (EVs) that are derived from stem cells are devoid of these issues and exhibit therapeutic effects that are comparable to those of their parent

Received: 9 March 2024. **Revised:** 1 September 2024. **Accepted:** 21 January 2025

stem cells. Moreover, EVs are easily bioengineered and are considered ideal drug carriers [14, 15]. Consequently, stem-cell-derived EVs have attracted considerable attention as an ideal alternative to stem-cell-based therapy [16].

Bone marrow mesenchymal stem cells (BM-MSCs) are a major source of human stem cells [17] and the therapeutic potential of BM-MSCs in various diseases has been well recognized [18, 19]. In particular, both BM-MSCs and their secreted extracellular vesicles (BM-MSC-EVs) have been found to exert a protective effect against II/R-triggered injury. For instance, submucosal infusion of BM-MSCs in rats protects the intestinal mucosa against II/R injury [20]. BM-MSC-EVs can alleviate II/R-induced lung injury through the TLR4/NF-κB pathway [21]. Additionally, BM-MSC-EVs can attenuate II/R damage by regulating pyroptosis [22]. However, the precise mechanisms behind this protective effect remain incompletely comprehended.

The ubiquitin system controls a diverse array of biological processes, both physiologically and pathologically [23]. One crucial function of ubiquitination is to label targeted proteins for degradation by the proteasome [24]. Ubiquitination is achieved by the E1 ubiquitin-activating enzyme, E2 ubiquitin-conjugating enzymes, and E3 ubiquitin ligases [25]. This process can be reversed by deubiquitinases, such as ubiquitin-specific proteases (USPs) [26].

Accumulating evidence has demonstrated the essential role of ubiquitination regulators in II/R. For instance, inhibition of the E1 ubiquitin-activating enzyme protects organs against II/R injury by attenuating the NF-κB pathway [27]. The E3 ligase TRIM65 reduces II/R injury by inhibiting TOX4-mediated apoptosis [28]. Furthermore, USP22 promotes the proliferation and regeneration of damaged intestinal tissues in the context of II/R [29]. Nevertheless, considering their large number, the specific roles of other ubiquitination regulators in II/R and their downstream targets remain elusive.

In this study, we screened for differentially expressed USPs in IEC-6 intestinal epithelial cells following oxygen-glucose deprivation/reperfusion (OGD/R) treatment. Our observations revealed a significant downregulation of USP38 in OGD/R-treated IEC-6 cells and the expression of USP38 in these cells was markedly induced by the treatment with BM-MSC-EVs. Subsequently, we examined the impact of elevated USP38 levels on OGD/R-treated IEC-6 cells and explored the underlying mechanism.

Materials and methods

Characterization of BM-MSCs

The isolation of BM-MSCs was carried out by using IMMOCELL (Xiamen, Fujian, China). These cells were isolated from 28-day-old Wistar rats by following a previously established protocol [30]. Briefly, the bone marrow cavities of the tibia and femur were irrigated with 5 mL of alpha-minimum essential medium (α-MEM; #12571063, Gibco, Waltham, MA, USA) by using a syringe. The resulting cell suspension was filtered through a 200-mesh nylon filter and centrifuged at 115 *g* for 10 min at room temperature. The isolated cells were cultured in α-MEM that was supplemented with 10% fetal bovine serum (FBS; #10099158, Gibco), 100 μg/mL of streptomycin, and 100 U/mL of penicillin. Subsequently, the cells were analysed by using a NovoCyte FACS cytometer (Agilent, Santa Clara, CA, USA) to confirm their characteristic features as BM-MSCs. The antibodies that were used for this analysis, including CD14 (#325603; 1:100), CD19 (#302205; 1:100), CD34 (#343503; 1:100), CD45 (#304005; 1:100), CD44 (#397517; 1:100), CD73 (#344016; 1:100), CD90 (#328107; 1:100), and CD105 (#323204; 1:100), were purchased from BioLegend (San Diego, CA, USA).

The pluripotent capacity of the BM-MSCs was verified through the induction of differentiation into osteocytes, chondrocytes, or adipocytes, by using the STEMPRO® Osteogenesis Differentiation Kit (#A1007201, Thermo Fisher Scientific, Waltham, MA, USA), Chondrogenesis Differentiation Kit (#A1007101, Thermo Fisher Scientific), and Adipogenesis Differentiation Kit (#A1007001, Thermo Fisher Scientific), respectively.

Alizarin red, alcian blue, and oil red staining

The isolated BM-MSCs were induced for 2 weeks, followed by washing with phosphate buffered saline (PBS) and fixation with 4% paraformaldehyde for 30 min. Subsequently, the cells were rinsed with PBS and subjected to alizarin red, alcian blue, or oil red staining to assess their differentiation potential into osteocytes, chondrocytes, or adipocytes.

For alizarin red staining, the fixed cells were treated with 60% isopropanol for 1 min at room temperature, followed by PBS washing thrice and incubation with a 10% alizarin red solution for 15 min at room temperature. Finally, the stained cells were washed with PBS.

For alcian blue staining, the fixed cells were incubated with a solution containing 1% alcian blue and 0.1 N HCl for 30 min at room temperature, followed by thrice washing with 0.1 N HCl. Finally, the stained cells were immersed in ddH_2O.

For oil red staining, the fixed cells were incubated with a 0.5% oil red/isopropanol solution for 5 min at 37°C in the dark. Subsequently, the staining solution was removed and the cells were washed with ddH_2O.

All stained cells were observed and documented by using an Axio Imager M2 microscope that was equipped with a digital camera (Carl Zeiss AG, Oberkochen, Baden-Württemberg, Germany).

Plasmid construction

All USP overexpression plasmids were sourced from Anti-Hela Biotechnology (Xiamen, Fujian, China) and underwent sequencing for validation. The primers that were used to construct the other plasmids are detailed in Supplementary Table S1. Transfection experiments were conducted by using Lipofectamine 2000 reagent (Invitrogen, Waltham, MA, USA).

Purification and characterization of BM-MSC-EVs

The conditioned medium from BM-MSCs was utilized for EV purification. Initially, media from multiple culture batches were pooled and subjected to centrifugation at 2,000 *g* for 30 min at 4°C. Subsequently, this supernatant underwent centrifugation at 10,000 *g* for 30 min at 4°C, and the resulting supernatant was filtered through 0.45-μm syringe filters. Next, the filtered supernatant was further centrifuged at 100,000 *g* for 70 min at 4°C and the resulting pellet was resuspended in ice-chilled PBS, followed by filtration through 0.22-μm syringe filters. Afterward, the supernatant was centrifuged at 100,000 *g* for another 70 min at 4°C. Finally, the supernatant was discarded and the centrifuged pellet was resuspended in 100 μL of ice-chilled PBS.

Two aliquots of 5 μL were utilized for transmission electron microscopy (TEM) analysis or nanoparticle tracking analysis (NTA) to observe the morphology and measure the size of the purified EVs, respectively. Another aliquot of 5 μL was employed for Western blot to evaluate the presence of EV markers, including

CD9, CD81, and CD63. The unused EVs were stored at −80°C for subsequent experiments.

Western blot

The cells were lysed and total protein was extracted by using RIPA buffer supplemented with protease inhibitors (TIANGEN Biotechnology, Beijing, China). The protein concentration was measured by using a bicinchoninic acid assay (BCA) kit (TIANGEN Biotechnology). Next, the samples were denatured at 95°C for 5 min and separated by using 10% sodium dodecyl sulfate polyacrylamide gel electrophoresis (SDS-PAGE) gels, followed by transfer onto polyvinylidene fluoride or polyvinylidene difluoride (PVDF) membranes. Subsequently, the membranes were blocked by using 5% non-fat milk/TBST (TBS + 0.1% Tween 20) for 60 min, followed by overnight incubation with primary antibody solutions at 4°C. The next day, the membranes were washed with TBST and then incubated with secondary antibody solutions for 60 min at room temperature. Finally, the membranes were washed with TBST and subjected to signal development by using an enhanced chemiluminescence (ECL) kit (Proteintech, Wuhan, Hubei, China). The signals were visualized and documented by using a ChemiDoc machine (Bio-Rad, Hercules, CA, USA). The resulting images were quantified for the intensity of the protein bands by using ImageJ (NIH, Bethesda, MD, USA). The antibodies for Western blot and their dilutions are listed in Supplementary Table S2.

Cell culture and OGD/R treatment

293T cells (#IM-H222) and IEC-6 cells (#IM-R008) were procured from IMMOCELL and maintained in DMEM medium (#11965092; Gibco) that was supplemented with 10% FBS.

To establish the OGD/R model, IEC-6 cells were cultured until reaching 80% confluence. Subsequently, the medium was replaced with D-Hanks' buffer (Sigma-Aldrich, Burlington, MA, USA) and cells were cultured in an incubator filled with 95% N_2 and 5% CO_2 for 4 h at 37°C. Following this, the cells were cultured in the normal medium under standard conditions for 3, 6, 12, or 24 h. The term "mock" refers to cells without OGD/R treatment.

CCK-8 assay

The assessment of cell viability was conducted by using a CCK-8 assay kit (MedChemExpress, Monmouth Junction, NJ, USA). Briefly, IEC-6 cells were seeded into 96-well plates and cultured for 12 h. Subsequently, the cells were incubated with the CCK-8 working reagents for 2 h at room temperature in the dark. Finally, the OD_{510} values of each well were measured and documented for statistical analysis. Each sample was tested in triplicate and three samples of each treatment were assayed.

Annexin V/PI staining

An annexin V/PI staining kit (Beyotime Biotechnology, Haimen, Jiangsu, China) was utilized to evaluate cell apoptosis. In brief, the cells were digested and pelleted, followed by incubation with the working solution mixed with PI staining solution and 1:20 diluted annexin V-FITC/PBS in the dark for 15 min at room temperature. Finally, the samples were analysed by using flow cytometry.

Transwell assay

The transwell assay was employed to evaluate cell migration. A total of 8×10^4 cells were seeded into each well of the upper compartment of transwell chambers with a pore size of 8 μm (Corning, NY, USA), supplemented with serum-free culture medium. The lower compartment was filled with 500 μL of DMEM medium that was supplemented with 10% FBS, 100 μg/mL of streptomycin, and 100 U/mL of penicillin. After culturing at 37°C for 24 h, the upper chambers were washed with PBS. Subsequently, cells on the lower surface of the transwell membranes were fixed with 95% ethanol for 10 min, followed by staining with a 0.1% crystal violet solution for another 10 min. Finally, the membranes were washed with PBS, air-dried, and imaged. Image J was used to quantify the cell number. Each condition was tested three independent times.

EV tracing

The carboxyfluorescein succinimidyl ester (CFSE) dye (#40714ES76; Yeasen, Shanghai, China) was utilized to label BM-MSC-EVs at a dilution of 1:1000. After incubation at 37°C for 2 h, the labeled EVs were combined with IEC-6 cells for the specified duration. Subsequently, the cells were washed with PBS and subjected to observation and imaging by using an Axio Imager M2 microscope.

Quantitative polymerase chain reaction

Total RNA extraction was performed by using the RNAiso Plus reagent (Takara, Kusatsu, Shiga, Japan). Complementary DNA (cDNA) synthesis was conducted by using the PrimeScript II RTase kit (Takara). Subsequently, quantitative polymerase chain reaction (qPCR) was executed by utilizing the Tli RNase H Plus (Takara) on a QuantStudio Real-Time PCR system (Thermo Fisher Scientific). The expression levels of the target genes were assessed by using the $2^{-\Delta\Delta Cq}$ algorithm. The qPCR primers can be found in Supplementary Table S3.

DCFDA staining

The assessment of cellular ROS levels was conducted by using a DCFDA staining kit (#ab113851; Abcam, Cambridge, UK). Briefly, IEC-6 cells were stained with DCFDA for 30 min at 37°C in the dark. Subsequently, the cells were washed and seeded into microplates at a density of 10^5 cells per well. Finally, the plates underwent flow cytometry analysis and the median fluorescence intensity of each well was recorded, normalized, and calculated.

Co-IP

Cells that were transfected with HA-USP38 and/or Flag-BIRC5 were cultured for 48 h. Subsequently, the cells were pelleted and lysed by using an IP buffer followed by sonication on ice for 15 min. After centrifugation, the resulting supernatants were incubated with beads that were conjugated with HA-tag or Flag-tag antibodies at room temperature for 2 h. Finally, the proteins that were bound to the beads were eluted and subjected to Western blot analysis.

Statistical analysis

Statistical analysis and graph generation were performed by using Prism v8.0 (GraphPad, La Jolla, CA, USA). Significance between two specified datasets was assessed by using an unpaired two-tailed Student's *t*-test, while significance among three datasets was determined by using one-way analysis of variance. A *P*-value of <0.05 was considered statistically significant.

Results

Establishment of a cell model for II/R

To investigate whether USPs regulate II/R, we initially treated IEC-6 cells with 4 h of OGD and 3, 6, 12, or 24 h of reperfusion to optimize the OGD/R condition for constructing an II/R cell model. Subsequently, we assessed the viability of the OGD/R-treated cells. CCK-8 staining data revealed that IEC-6 cells that were

treated with 6 h of reperfusion following 4 h of OGD exhibited ~50% viability relative to OGD cells without reperfusion (Supplementary Figure S1A). Consistently, the apoptosis of IEC-6 treated with OGD with 6 h of reperfusion was substantially elevated compared with that of untreated cells, as evidenced by the annexin V/PI staining results (Supplementary Figure S1B and C). Moreover, the migration of IEC-6 cells was remarkably attenuated upon treatment of OGD with 6 h of reperfusion, as indicated by the transwell assay outcomes (Supplementary Figure S1D and E). The results suggest that treatment of IEC-6 cells with 4 h of OGD and 6 h of reperfusion (hereafter referred to as OGD/R for convenience) can serve as a cell model for II/R.

USP38 expression was downregulated in OGD/R-treated IEC-6 cells

Subsequently, we conducted qPCR to assess the expression of 38 USPs in mock-treated and OGD/R-treated IEC-6 cells. The results indicated that USP38, USP21, and USP30 are the most significantly downregulated USPs upon OGD/R treatment (Figure 1A). However, Western blot data revealed that only USP38, not USP21 or USP30, exhibited a noticeable decrease in OGD/R-treated IEC-6 cells (Figure 1B and C). To determine the impact of these USPs on OGD/R-treated IEC-6 cells, we overexpressed USP38, USP30, or USP21 in OGD/R-treated IEC-6 cells (Figure 1D) and assessed their viability. CCK-8 staining data uncovered that excessive USP38 and USP30 could significantly rescue the impaired viability of IEC-6 cells upon OGD/R treatment, whereas USP21 had no such effect (Figure 1E). These findings indicate that USP38 may exert a protective effect on IEC-6 cells against OGD/R-triggered injury.

USP38 in BM-MSC-EVs alleviated OGD/R-induced injury in IEC-6 cells

As BM-MSC-EVs have demonstrated the ability to alleviate II/R injury, we investigated whether USP38 mediates the protective

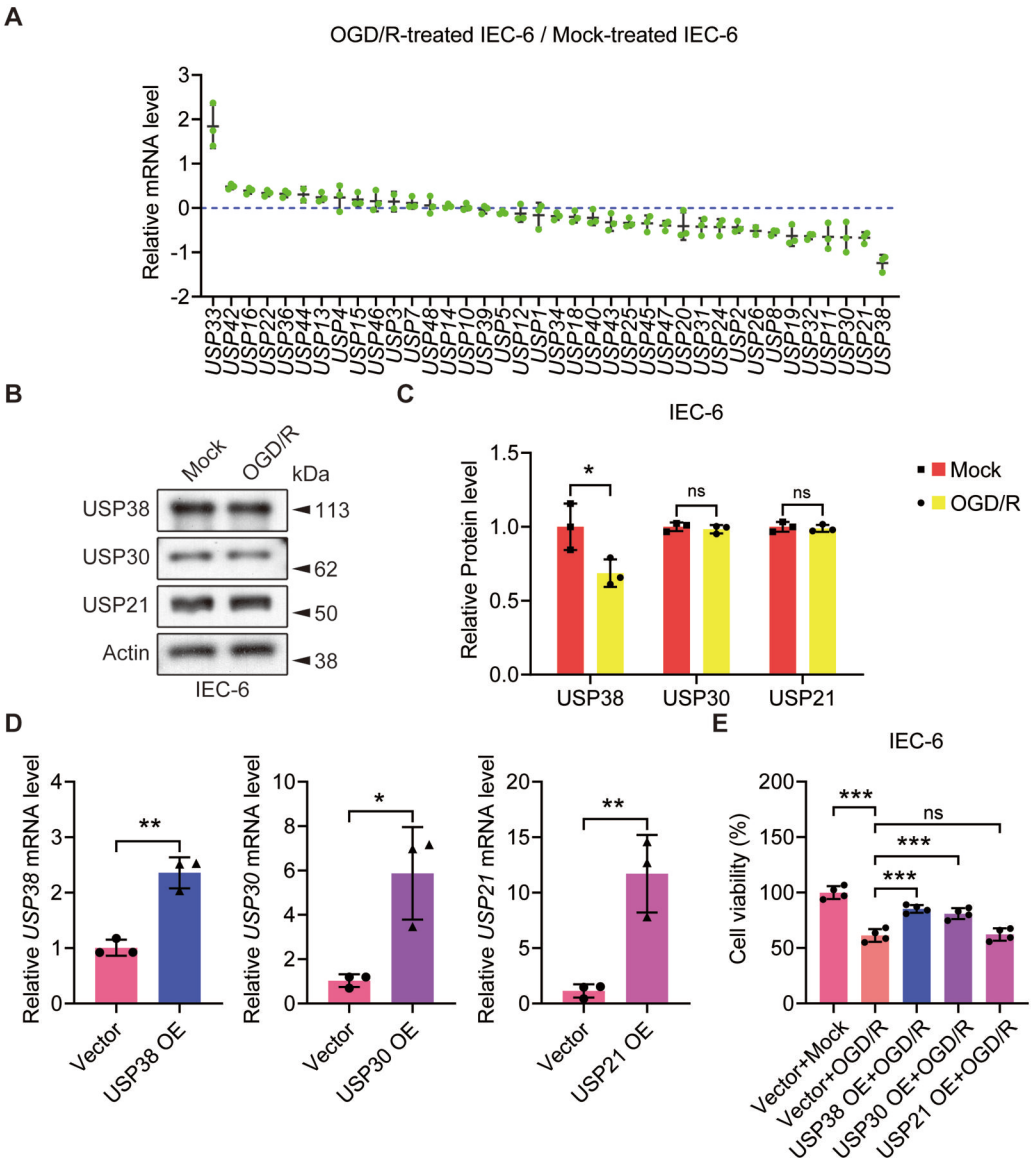

Figure 1. USP38 expression was downregulated in OGD/R-treated IEC-6 cells. (A) qPCR data show that the expression of USP38, USP21, and USP30 is significantly downregulated in OGD/R-treated IEC-6 cells. The values represent the ratio of the expression of individual USPs in OGD/R-treated and mock-treated cells. (B) Western blot data reveal a significant reduction in USP38 expression upon OGD/R treatment in IEC-6 cells, while the expression of USP30 and USP21 remains unaltered. (C) Quantification data from the Western blot results. (D) qPCR results confirm the overexpression of USP38, USP30, and USP21 in IEC-6 cells. (E) CCK-8 staining results indicate that excessive USP38 and USP30 improve the impaired viability caused by OGD/R treatment, while overexpression of USP21 has no such effect. The data are presented as mean ± standard deviation. *$P < 0.05$; **$P < 0.01$; ***$P < 0.001$; ns = no significant difference.

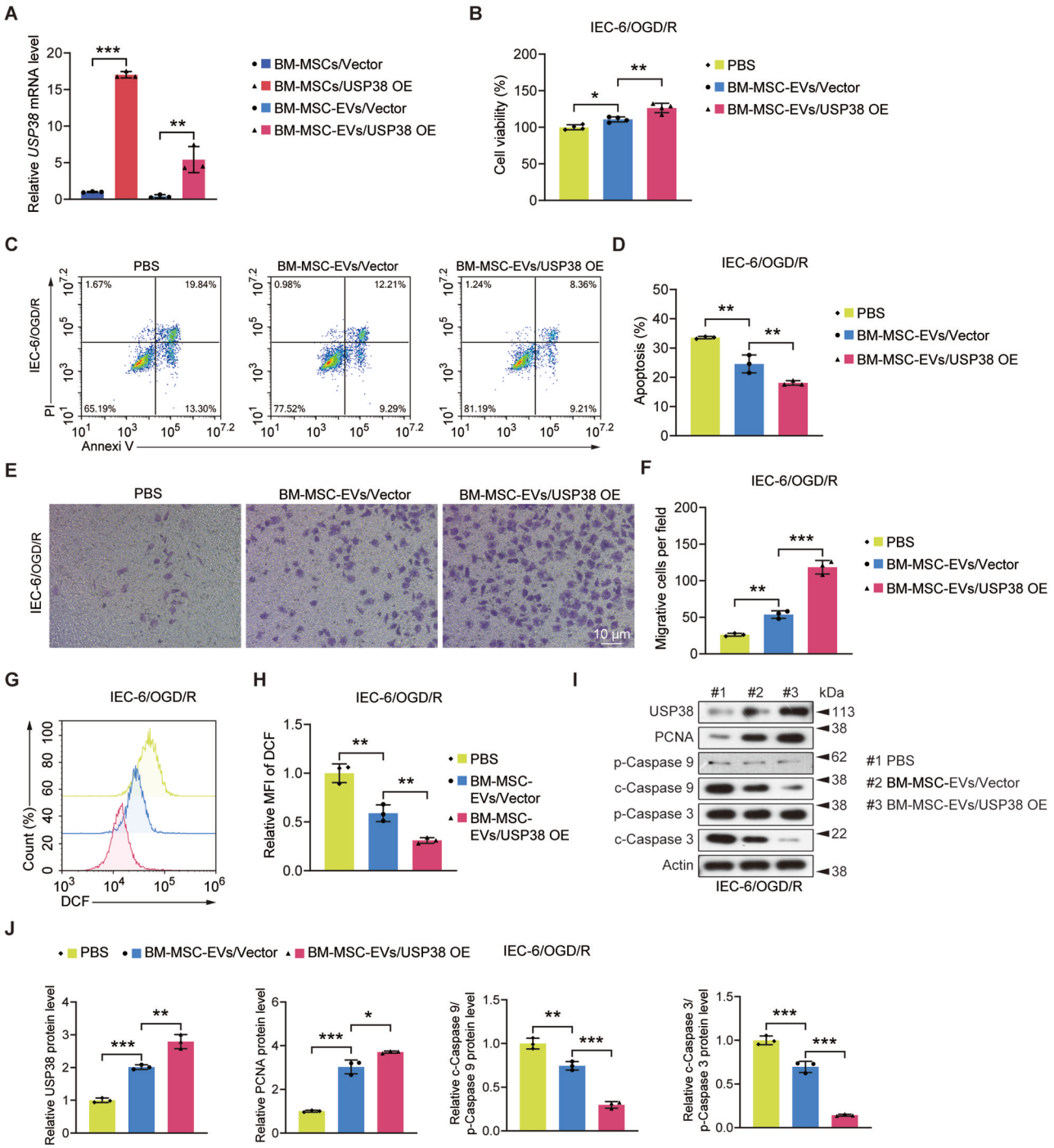

Figure 2. USP38 in BM-MSC-EVs alleviated the OGD/R-triggered injury in IEC-6 cells. (A) qPCR data demonstrate the successful overexpression of USP38 in BM-MSCs and their secreting EVs. (B) CCK-8 staining reveals that BM-MSC-EVs increase the viability of OGD/R-treated IEC-6 cells and this effect is enhanced by USP38 overexpression. (C) Annexin V/PI staining outcomes uncover that BM-MSC-EVs reduce the apoptosis of OGD/R-treated cells and excessive USP38 strengthens this effect. (D) Quantification of the annexin V/PI staining data presented in (C). (E) Transwell assay results indicate that excessive USP38 enhances the pro-migratory function of BM-MSC-EVs on OGD/R-treated IEC-6 cells. (F) Quantification of the transwell assay results. (G) DCFDA staining results show that USP38 overexpression potentiates the antioxidant effect of BM-MSC-EVs on OGD/R-treated IEC-6 cells. (H) Quantification of the data shown in (G). (I) Western blot data indicate that incubation of BM-MSC-EVs with OGD/R-treated cells results in increased levels of USP38 and PCNA, and decreased levels of c-caspase 9 and c-caspase 3. This effect is enhanced by USP38 overexpression. (J) Quantification of the Western blot data. The data are presented as mean ± standard deviation. *$P < 0.05$; **$P < 0.01$; ***$P < 0.001$. OE = overexpression.

function of BM-MSC-EVs on OGD/R-treated IEC-6 cells. To address this question, we initially isolated rat BM-MSCs and characterized their stemness and pluripotency. Flow cytometry analysis revealed that the cells did not express hematopoietic cell markers CD14, CD19, CD34, or CD45, but did express MSC surface markers CD44, CD73, CD90, and CD105 (Supplementary Figure S2A). Subsequently, we induced these cells to undergo osteogenic, chondrogenic, or adipogenic differentiation by using specified media. Results from alizarin red, alcian blue, and oil red staining confirmed their capability to differentiate into osteocytes, chondrocytes, or adipocytes (Supplementary Figure S2B), establishing the identity of the isolated cells as BM-MSCs.

Following this, we collected conditioned media from these cells and purified the secreted EVs. TEM and NTA analyses confirmed that the purified EVs displayed typical EV morphology and size (Supplementary Figure S2C and D) and were enriched in the expression of EV surface markers CD9, CD81, and CD63 (Supplementary Figure S2E). These observations affirm the successful purification of BM-MSC-EVs.

To assess whether BM-MSC-EVs can be absorbed by OGD/R-treated IEC-6 cells, we labeled these EVs with CFSE and incubated them with the cells for 24 or 48 h. Our observations indicated that the labeled EVs were incorporated into the cells in a time-dependent manner (Supplementary Figure S3A). Annexin V/PI staining and transwell assay data revealed that, after 48 h of incubation with BM-MSC-EVs, OGD/R-treated IEC-6 cells exhibited a significant reduction in apoptosis and enhanced migration (Supplementary Figure S3B–E).

Subsequently, we overexpressed USP38 in BM-MSCs and purified their EVs. qPCR results confirmed the overexpression of USP38 in both BM-MSCs and their EVs (Figure 2A). CCK-8 staining results revealed that overexpression of USP38 in BM-MSC-EVs significantly enhanced their ability to promote the viability of OGD/R-treated IEC-6 cells (Figure 2B). Additionally, the anti-apoptotic effect of BM-MSC-EVs on OGD/R-treated IEC-6 cells was strengthened by excessive USP38, as evidenced by the annexin V/PI staining outcomes (Figure 2C and D). Furthermore, transwell assay data showed that the pro-migratory function of BM-MSC-EVs on OGD/R-treated IEC-6 cells was enhanced by USP38 overexpression (Figure 2E and F). Additionally, DCFDA staining data uncovered that excessive USP38 strengthened the ability of BM-MSC-EVs to reduce the ROS level in OGD/R-treated IEC-6 cells (Figure 2G and H). At the molecular level, Western blot data revealed that incubation with control BM-MSC-EVs alone significantly elevated the expression of USP38 and proliferating cell nuclear antigen (PCNA), a proliferation marker, while repressing the expression of pro-apoptotic markers c-caspase 9 and c-caspase 3 in OGD/R-treated IEC-6 cells. This effect was more pronounced in OGD/R-treated IEC-6 cells that were incubated with USP38-overexpressing BM-MSC-EVs (Figure 2I and J). Collectively, these findings indicate that BM-MSC-EVs can upregulate USP38 expression in IEC-6 cells that are treated with OGD/R, and excessive USP38 potentiates the protective effect of BM-MSC-EVs on IEC-6 cells against OGD/R-triggered injury.

USP38 interacted with and deubiquitinated BIRC5 in IEC-6 cells

To delineate the mechanism by which USP38 protects OGD/R-treated IEC-6 cells, we screened USP38-interacting proteins by using the BioGRID database [31] and focused on proteins that are known for their function in regulating intestinal homeostasis. Among these, BIRC5 is a key regulator of the proliferation and apoptosis of intestinal epithelial cells [32]. Therefore, we investigated whether USP38 can affect the stability of BIRC5 in IEC-6 cells. Co-IP assay data showed that USP38 can interact with BIRC5 (Figure 3A) and the overexpression of USP38 in IEC-6 cells

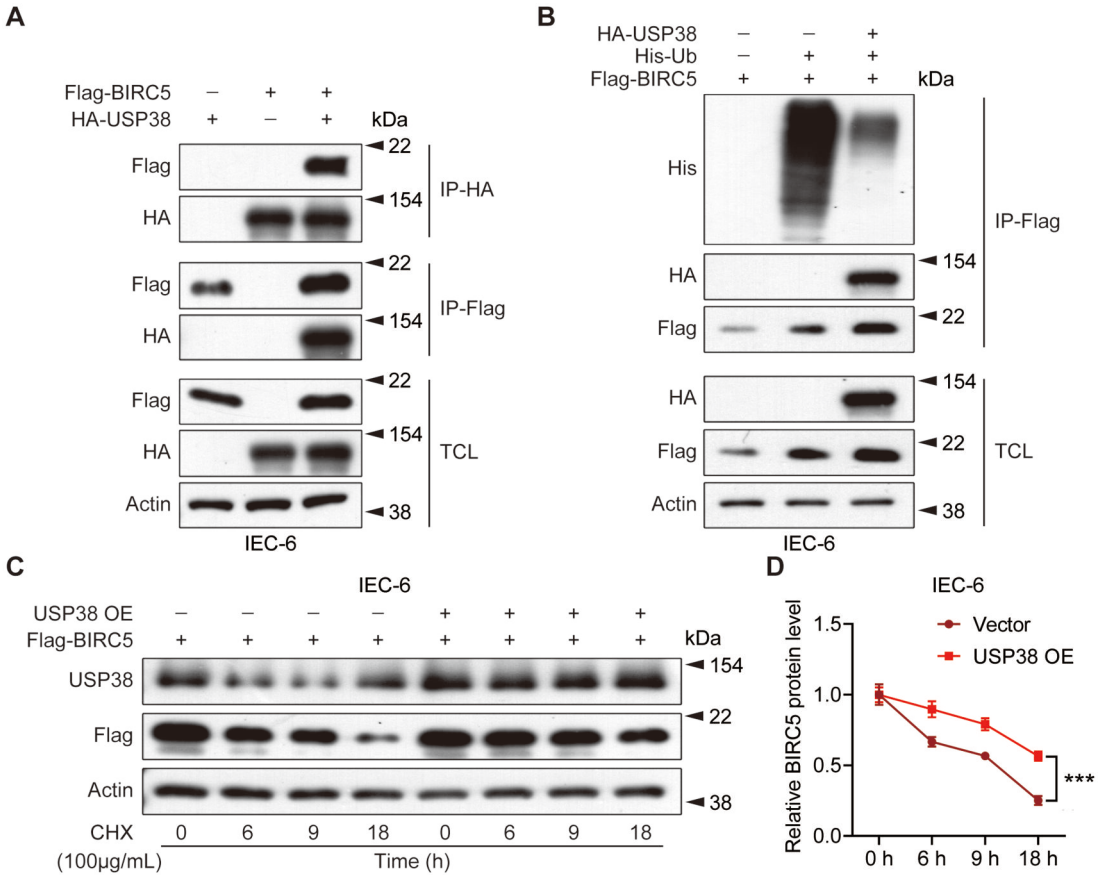

Figure 3. USP38 interacted with and deubiquitinated BIRC5 in IEC-6 cells. (A) Co-IP data demonstrate the interaction between BIRC5 and USP38 in IEC-6 cells. (B) Co-IP results reveal that excessive USP38 significantly reduces the ubiquitination level of BIRC5 in IEC-6 cells. (C) Western blot data uncover that overexpression of USP38 stabilizes BIRC5 in IEC-6 cells. (D) Quantification of the data shown in (C). The data are presented as mean ± standard deviation. ***$P < 0.001$. All these experiments were repeated three times. TCL = total cell lysate, OE = overexpression, IP = immunoprecipitation, CHX = cycloheximide.

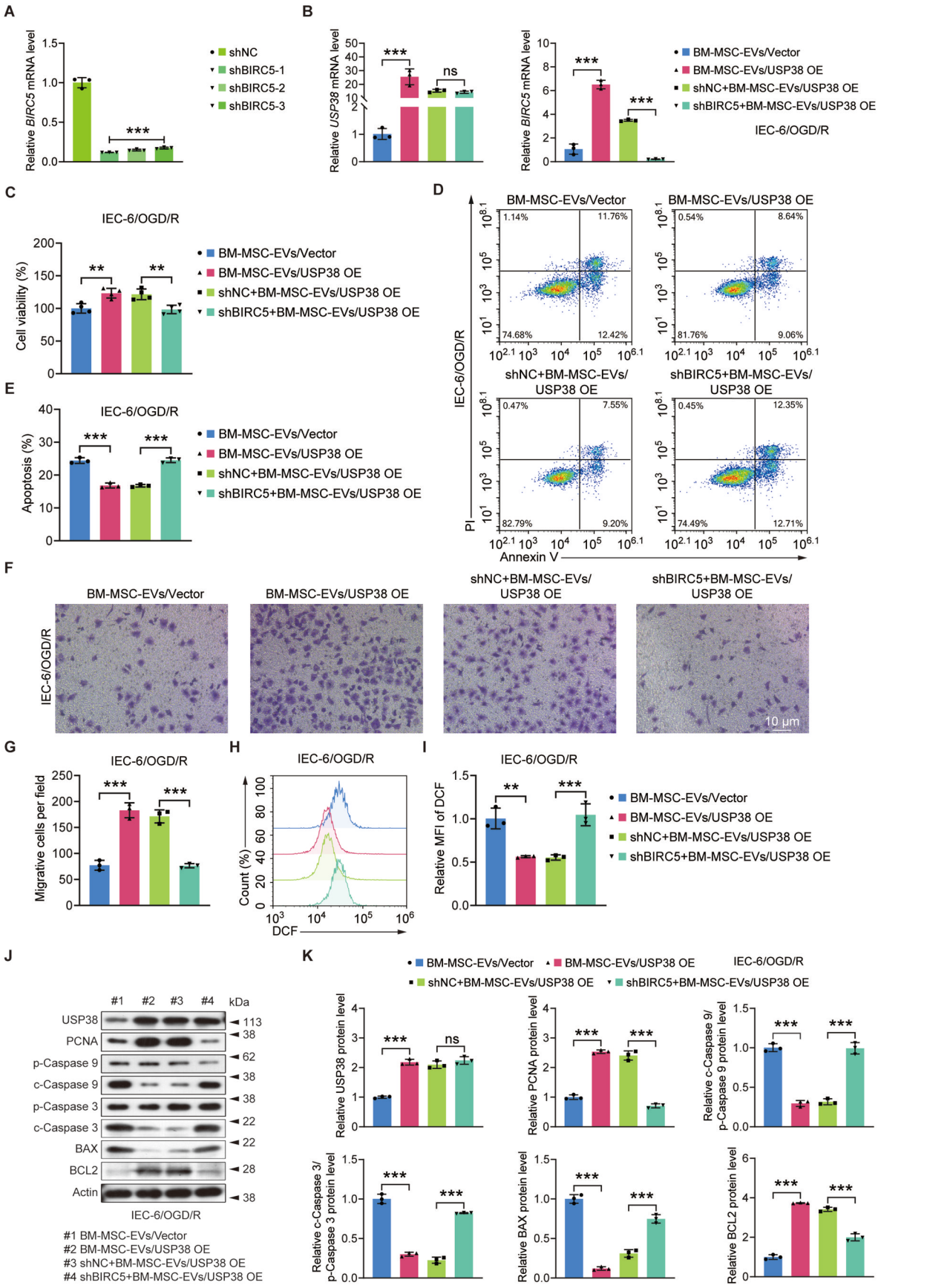

Figure 4. BIRC5 mediated the protective effect of USP38 in protecting IEC-6 cells from OGD/R-triggered injury. (A) qPCR data demonstrate the efficient depletion of BIRC5 expression in IEC-6 cells by all three shBIRC5s. (B) qPCR results reveal that USP38-overexpressing BIRC5-deficient BM-MSC-EVs elevate USP38 and reduce BIRC5 expression in OGD/R-treated IEC-6 cells. (C) CCK-8 staining data uncover that BIRC5 knock-down abolishes the

(Continued)

significantly decreased the ubiquitination level of BIRC5 (Figure 3B). Furthermore, we treated BIRC5-overexpressing IEC-6 cells with the protein synthesis inhibitor cycloheximide (CHX) and transfected control or USP38-overexpression plasmids. Western blot data revealed that USP38 significantly enhanced the stability of BIRC5 (Figure 3C and D). These results suggest that USP38 interacts with and deubiquitinates BIRC5 to stabilize it in IEC-6 cells.

USP38 protected IEC-6 cells from OGD/R-induced injury by stabilizing BIRC5

To determine whether USP38 stabilizes BIRC5 to protect OGD/R-treated IEC-6 cells, we constructed BIRC5-deficient USP38-overexpressing BM-MSCs and purified their EVs. All three shRNAs that were targeting BIRC5 efficiently depleted BIRC5 in 293 T cells (Figure 4A), as indicated by qPCR results. We selected shBIRC5-1 in the subsequent experiments, as it exhibited the highest efficiency in knocking down BIRC5. qPCR data confirmed that incubation of BIRC5-deficient USP38-overexpressing BM-MSC-EVs could efficiently increase USP38 and reduce BIRC5 expression in OGD/R-treated IEC-6 cells (Figure 4B). CCK-8 staining, annexin V/PI staining, and transwell assay results revealed that the strengthened pro-proliferative, anti-apoptotic, and pro-migratory effects of BM-MSC-EVs on OGD/R-treated IEC-6 cells by USP38 overexpression were abolished by BIRC5 knock-down (Figure 4C–G). Moreover, BIRC5 deficiency also nullified the effect of excessive USP38 in decreasing the ROS level of OGD/R-treated IEC-6 cells, as evidenced by the DCFDA staining results (Figure 4H and I). Molecularly, the increased expression of PCNA and reduced levels of c-caspase 9 and c-caspase3 by USP38 overexpression in OGD/R-treated IEC-6 cells were mitigated by BIRC5 deficiency. Conversely, the downregulated expression of another pro-apoptotic regulator BAX and the elevated expression of the anti-apoptotic marker BCL2, which was caused by excessive USP38, were reversed by BIRC5 knock-down (Figure 4J and K). Taken together, these findings suggest that BIRC5 plays an essential role in mediating the protective effect of USP38 on OGD/R-treated IEC-6 cells.

Discussion

I/R can occur in various organs and tissues. Although reperfusion is necessary for the survival of ischemic tissue, the damage that is triggered by increased blood flow and high levels of oxygen is more severe than that caused by ischemia [33]. Therefore, having a more comprehensive understanding of the mechanisms that protect tissues from I/R-triggered injury is critical for the development of novel therapies to treat conditions such as II/R. In this study, we investigated the role of USP38 in an II/R cell model. Our data provide direct evidence that USP38 exhibits a protective function on OGD/R-treated IEC-6 cells.

USP38 is a deubiquitinase that regulates a diverse array of substrates, influencing various biological processes. For instance, USP38 acts as a tumor suppressor in colorectal cancer (CRC), with its expression downregulated in CRC cells. It negatively regulates the stemness and chemoresistance of CRC by deubiquitinating HDAC3 [34]. Conversely, in gastric cancer (GC), USP38 is overexpressed and promotes the proliferation and migration of GC cells, facilitating GC progression by stabilizing FASN [35]. USP38 also mitigates cerebral I/R-induced injury, with its expression downregulated in I/R-treated brain tissues. It ameliorates IR-induced neuroinflammation by upregulating KDM5B expression [36]. Consistently, our findings also demonstrate the protective role of USP38 in the II/R cell model. However, it is essential to validate these findings *in vivo*, and it would also be intriguing to explore whether USP38 can alleviate I/R-triggered injury in other contexts.

Considering the extensive number of USPs, it is plausible that additional USPs also contribute to the regulation of II/R. Supporting this notion, our data demonstrate that overexpression of USP21 significantly enhances the viability of OGD/R-treated IEC-6 cells, even though its protein level remains unchanged upon OGD/R treatment. However, whether USP21 can mitigate other damage that is caused by I/R remains unclear. These findings also imply that USPs, the expression of which is unaltered upon OGD/R treatment, may still play a role in regulating II/R. Further investigations are necessary to elucidate the precise roles of each USP in the context of II/R.

BIRC5, also known as Survivin, is a member of the inhibitors of apoptosis protein family and is generally recognized as an oncogene due to its anti-apoptotic and pro-proliferative roles [37]. Within the intestinal epithelium, BIRC5 plays a crucial role in maintaining the stem-cell niche and promoting the proliferation and survival of epithelial cells [32, 38]. Hence, mediation of the protective role of USP38 on OGD/R-treated IEC-6 cells by BIRC5 is not surprising, given its pro-proliferative and anti-apoptotic functions. However, it remains unclear whether BIRC5 expression is altered upon OGD/R treatment in intestinal epithelial cells and whether BIRC5 is the sole mediator of the protective function of USP38 in these cells.

The mechanism that regulates USP38 expression remains elusive. As mentioned earlier, USP38 expression is decreased in CRC cells and I/R-treated cerebral and IEC-6 cells but upregulated in GC cells. Our data reveal that, when OGD/R-treated IEC-6 cells were incubated with BM-MSC-EVs, their USP38 level significantly increased. One possibility for this upregulation is that USP38 mRNA that was enclosed in the BM-MSC-EVs was delivered into the IEC-6 cells. Alternatively, other ingredients that were encapsulated in these EVs may have stimulated the transcription and/or translation of USP38 in recipient IEC-6 cells.

The engineering and modification of EVs is a hot topic in the research on the clinical application of EVs [39, 40]. Although BM-MSC-EVs exhibit therapeutic potential in treating various diseases [41], the efficacy of these EVs could still be enhanced by proper modification [42]. In support of this, our findings demonstrate that overexpression of USP38 significantly enhances the protective function of BM-MSC-EVs on OGD/R-treated IEC-6 cells. Next, it will be intriguing to test whether the administration of such EVs can alleviate II/R injury *in vivo*.

Figure 4. Continued
pro-proliferative effect of USP38 on OGD/R-treated IEC-6 cells. (D) Annexin V/PI staining outcomes indicate that BIRC5 depletion mitigates the anti-apoptotic effect of excessive USP38 on OGD/R-treated IEC-6 cells. (E) Quantification of the data presented in (D). (F) Transwell assay results show that BIRC5 deficiency nullifies the pro-migratory function of excessive USP38 on OGD/R-treated IEC-6 cells. (G) Quantification of the data shown in (F). (H) DCFDA staining data uncover that the antioxidant effect of USP38 overexpression on OGD/R-treated IEC-6 cells is substantially attenuated by BIRC5 knock-down. (I) Quantification of the data presented in (H). (J) Western blot results show that excessive USP38 causes increased levels of PCNA and BCL2 and decreased expression of c-caspase 9, c-caspase 3, and BAX. However, this effect is abolished by BIRC5 deficiency. (K) Quantification of the Western blot data. The data are presented as mean ± standard deviation. $^{**}P < 0.01$; $^{***}P < 0.001$; ns = no significant difference, OE = overexpression.

In summary, we identified USP38 as a potent protector of intestinal epithelial cells from I/R-triggered injury by stabilizing BIRC5. Overexpression of USP38 substantially enhances the protective role of BM-MSC-EVs on II/R. These observations expand our knowledge about the function of USP38 and its substrate, and provide a potential strategy to treat II/R.

Supplementary data

Supplementary data is available at *Gastroenterology Report* online.

Authors' contributions

M.P. and J.L. conceived and designed the project; M.P., X.W.H., X. D.H., and X.L. collected the data; M.P., X.W.H., X.D.H., X.L., and J. L. analysed and interpreted the data; J.L. acquired funds and supervised the investigation; M.P. drafted the manuscript; All authors read and approved the final manuscript.

Funding

This work was supported by Natural Science Foundation of Fujian Province, China [2021J011357].

Conflicts of interest

The authors declare that they have no conflict of interest.

Data availability

The main data supporting the conclusions of this study are available within the article and its supplementary files.

References

1. Li G, Wang S, Fan Z. Oxidative stress in intestinal ischemia-reperfusion. *Front Med (Lausanne)* 2021;**8**:750731.
2. Nadatani Y, Watanabe T, Shimada S *et al.* Microbiome and intestinal ischemia/reperfusion injury. *J Clin Biochem Nutr* 2018; **63**:26–32.
3. Grootjans J, Lenaerts K, Derikx JP *et al.* Human intestinal ischemia-reperfusion-induced inflammation characterized: experiences from a new translational model. *Am J Pathol* 2010; **176**:2283–91.
4. Zhao W, Gan X, Su G *et al.* The interaction between oxidative stress and mast cell activation plays a role in acute lung injuries induced by intestinal ischemia-reperfusion. *J Surg Res* 2014; **187**:542–52.
5. Endean ED, Barnes SL, Kwolek CJ *et al.* Surgical management of thrombotic acute intestinal ischemia. *Ann Surg* 2001;**233**:801–8.
6. Günel E, Çağlayan F, Çağlayan O *et al.* Treatment of intestinal reperfusion injury using antioxidative agents. *J Pediatr Surg* 1998; **33**:1536–9.
7. Gutierrez-Sanchez G, Garcia-Alonso I, Gutierrez Saenz de Santa Maria J *et al.* Antioxidant-based therapy reduces early-stage intestinal ischemia-reperfusion injury in rats. *Antioxidants (Basel)* 2021;**10**:853.
8. Zamorano M, Castillo RL, Beltran JF *et al.* Tackling ischemic reperfusion injury with the aid of stem cells and tissue engineering. *Front Physiol* 2021;**12**:705256.
9. Arakawa M, Sakamoto Y, Miyagawa Y *et al.* iPSC-derived mesenchymal stem cells attenuate cerebral ischemia-reperfusion injury by inhibiting inflammatory signaling and oxidative stress. *Mol Ther Methods Clin Dev* 2023;**30**:333–49.
10. Barzegar M, Kaur G, Gavins FNE *et al.* Potential therapeutic roles of stem cells in ischemia-reperfusion injury. *Stem Cell Res* 2019; **37**:101421.
11. Shen ZY, Zhang J, Song HL *et al.* Bone-marrow mesenchymal stem cells reduce rat intestinal ischemia-reperfusion injury, ZO-1 downregulation and tight junction disruption via a TNF-alpha-regulated mechanism. *World J Gastroenterol* 2013;**19**:3583–95.
12. Liu L, He YR, Liu SJ *et al.* Enhanced effect of IL-1beta-activated Adipose-Derived MSCs (ADMSCs) on repair of intestinal ischemia-reperfusion injury via COX-2-PGE(2) signaling. *Stem Cells Int* 2020;**2020**:2803747.
13. Poulos J. The limited application of stem cells in medicine: a review. *Stem Cell Res Ther* 2018;**9**:1.
14. Tang Y, Zhou Y, Li HJ. Advances in mesenchymal stem cell exosomes: a review. *Stem Cell Res Ther* 2021;**12**:71.
15. Rao D, Huang D, Sang C *et al.* Advances in mesenchymal stem cell-derived exosomes as drug delivery vehicles. *Front Bioeng Biotechnol* 2021;**9**:797359.
16. Tan F, Li X, Wang Z *et al.* Clinical applications of stem cell-derived exosomes. *Signal Transduct Target Ther* 2024;**9**:17.
17. Hass R, Kasper C, Bohm S *et al.* Different populations and sources of human mesenchymal stem cells (MSC): A comparison of adult and neonatal tissue-derived MSC. *Cell Commun Signal* 2011;**9**:12.
18. Charbord P. Bone marrow mesenchymal stem cells: historical overview and concepts. *Hum Gene Ther* 2010;**21**:1045–56.
19. Pittenger MF, Discher DE, Peault BM *et al.* Mesenchymal stem cell perspective: cell biology to clinical progress. *NPJ Regen Med* 2019;**4**:22.
20. Jiang H, Qu L, Li Y *et al.* Bone marrow mesenchymal stem cells reduce intestinal ischemia/reperfusion injuries in rats. *J Surg Res* 2011;**168**:127–34.
21. Liu J, Chen T, Lei P *et al.* Exosomes released by bone marrow mesenchymal stem cells attenuate lung injury induced by intestinal ischemia reperfusion via the TLR4/NF-kappaB pathway. *Int J Med Sci* 2019;**16**:1238–44.
22. Wan Z, Zhang Y, Lv J *et al.* Exosomes derived from bone marrow mesenchymal stem cells regulate pyroptosis via the miR-143-3p/myeloid differentiation factor 88 axis to ameliorate intestinal ischemia-reperfusion injury. *Bioengineered* 2023;**14**:2253414.
23. Damgaard RB. The ubiquitin system: from cell signalling to disease biology and new therapeutic opportunities. *Cell Death Differ* 2021;**28**:423–6.
24. Zhao L, Zhao J, Zhong K *et al.* Targeted protein degradation: mechanisms, strategies and application. *Signal Transduct Target Ther* 2022;**7**:113.
25. Scheffner M, Nuber U, Huibregtse JM. Protein ubiquitination involving an E1-E2-E3 enzyme ubiquitin thioester cascade. *Nature* 1995;**373**:81–3.
26. Cruz L, Soares P, Correia M. Ubiquitin-specific proteases: players in cancer cellular processes. *Pharmaceuticals (Basel)* 2021; **14**:848.
27. Matsuo S, Chaung A, Liou D, *et al.* Inhibition of ubiquitin-activating enzyme protects against organ injury after intestinal ischemia-reperfusion. *Am J Physiol Gastrointest Liver Physiol* 2018; **315**:G283–92.
28. Huang Y, Chen T, Jiang M *et al.* E3 ligase TRIM65 alleviates intestinal ischemia/reperfusion injury through inhibition of TOX4-mediated apoptosis. *Cell Death Dis* 2024;**15**:29.
29. Ji AL, Li T, Zu G *et al.* Ubiquitin-specific protease 22 enhances intestinal cell proliferation and tissue regeneration after intestinal ischemia reperfusion injury. *World J Gastroenterol* 2019; **25**:824–36.

30. Li Z, Li Q, Tong K *et al.* BMSC-derived exosomes promote tendon-bone healing after anterior cruciate ligament reconstruction by regulating M1/M2 macrophage polarization in rats. *Stem Cell Res Ther* 2022;**13**:295.
31. Oughtred R, Rust J, Chang C *et al.* The BioGRID database: A comprehensive biomedical resource of curated protein, genetic, and chemical interactions. *Protein Sci* 2021;**30**:187–200.
32. Martini E, Wittkopf N, Gunther C *et al.* Loss of survivin in intestinal epithelial progenitor cells leads to mitotic catastrophe and breakdown of gut immune homeostasis. *Cell Rep* 2016;**14**:1062–73.
33. Hammerman C, Kaplan M. Ischemia and reperfusion injury. The ultimate pathophysiologic paradox. *Clin Perinatol* 1998;**25**:757–77.
34. Zhan W, Liao X, Liu J *et al.* USP38 regulates the stemness and chemoresistance of human colorectal cancer via regulation of HDAC3. *Oncogenesis* 2020;**9**:48.
35. Zheng Z, Shang Y, Xu R *et al.* Ubiquitin specific peptidase 38 promotes the progression of gastric cancer through upregulation of fatty acid synthase. *Am J Cancer Res* 2022;**12**:2686–96.
36. Wang H, Xue X. USP38 protein alleviates neuroinflammation of cerebral ischemia–reperfusion injury via KDM5B expression. *Mol Cell Toxicol* 2021;**17**:465–73.
37. Frazzi R. BIRC3 and BIRC5: multi-faceted inhibitors in cancer. *Cell Biosci* 2021;**11**:8.
38. Martini E, Schneider E, Neufert C *et al.* Survivin is a guardian of the intestinal stem cell niche and its expression is regulated by TGF-beta. *Cell Cycle* 2016;**15**:2875–81.
39. Liang Y, Duan L, Lu J *et al.* Engineering exosomes for targeted drug delivery. *Theranostics* 2021;**11**:3183–95.
40. Sadeghi S, Tehrani FR, Tahmasebi S *et al.* Exosome engineering in cell therapy and drug delivery. *Inflammopharmacology* 2023;**31**:145–69.
41. Tsiapalis D, O'Driscoll L. Mesenchymal stem cell derived extracellular vesicles for tissue engineering and regenerative medicine applications. *Cells* 2020;**9**:991.
42. Ulpiano C, da Silva CL, Monteiro GA. Bioengineered mesenchymal-stromal-cell-derived extracellular vesicles as an improved drug delivery system: methods and applications. *Biomedicines* 2023;**11**:1231.

Gastroenterology Report, 2025, 13, –
https://doi.org/10.1093/gastro/goaf024
Original Article